Journal of Power Sources 204 (2012) 74–78

Contents lists available at SciVerse ScienceDirect

Journal of Power Sources

journal homepage: www.elsevier.com/locate/jpowsour

Short communication

Durability of sulfonated polyimide membrane in humidity cycling for fuel cell applications

Kenji Miyatake [a,b,*], Hiroshi Furuya [a], Manabu Tanaka [b], Masahiro Watanabe [b,*]

[a] Clean Energy Research Center University of Yamanashi, 4 Takeda, Kofu, Yamanashi 400-8510, Japan
[b] Fuel Cell Nanomaterials Center, University of Yamanashi, 4 Takeda, Kofu, Yamanashi 400-8510, Japan

ARTICLE INFO

Article history:
Received 11 November 2011
Received in revised form
16 December 2011
Accepted 19 December 2011
Available online 29 December 2011

Keywords:
Sulfonated polyimide
Humidity cycling
Gas permeability
Membrane degradation
Mechanical failure

ABSTRACT

An aromatic proton conductive polymer, sulfonated polyimide copolymer membrane, was tested in humidity cycling under the conditions simulating fuel cell operation. The membrane was exposed periodically (every 2 min) to dry (nominal 0% relative humidity) and wet (100% relative humidity) at 80 °C, similar to the United States Department of Energy (US DOE) protocol for proton exchange membrane fuel cells. The membrane was durable for 10,000 cycles without mechanical failure. Post-test analyses by ^{1}H NMR spectra and gel permeation chromatography (GPC) revealed that the membrane was hydrolyzed to some extent during the cycling test while mechanical properties and gas impermeability were only slightly deteriorated.

1. Introduction

Fuel cells have attracted considerable interest as clean and efficient energy devices to produce electric power via electrochemical reaction of fuels and oxidants. Among different kinds of fuel cells, polymer electrolyte membrane fuel cells (PEMFCs) using proton exchange polymer membranes are most suitable for the applications to portable devices, residential uses, and electric vehicles [1,2]. Recent announcement by major car companies about the commercialization of fuel cell electric vehicles as of the year of 2015 has further prompted research and development of durable and cost-effective fuel cell materials. One of the most important components in PEMFCs is proton exchange membranes (PEMs). Perfluorosulfonic acid (PFSA) polymers composed of a perfluorocarbon polymer backbone with pendant perfluorosulfonic acid groups are state-of-the-art PEMs [3,4]. The perfluorinated structure combined with superacid groups provides excellent chemical stability as well as high proton conductivity. However, the high production cost and environmental incompatibility remain issues for such perfluorinated materials. Due to the synthetic complexity and difficulty, suppliers are very limited; Nafion of Du Pont, Aciplex of Asahi Kasei, Flemion of Asahi Glass, and Aquivion of Solvay Solexis. It is strongly desired to develop highly proton conductive and durable PEMs free from fluorine.

Hydrocarbon polymers with acidic functions have been investigated as alternative PEMs [5,6]. Especially, sulfonated aromatic polymers have been extensively explored in the last decade. Sulfonated polyimide (SPI) copolymers are among them. A number of research works have been conducted to optimize their chemical structure to fulfill the requirements as PEMs for fuel cells [7–14]. The parameters often considered include hydrophilicity and hydrophobicity of the comonomers, basicity and linearity of diamine monomers, copolymer composition, and sequenced block structure. Advantages of SPI membranes are very low gas permeability and high mechanical strength, and disadvantages are significant dependence of the proton conductivity on humidity and susceptibility to hydrolytic and oxidative degradation. Since SPIs are generally much more hygroscopic and absorb more water compared to the PFSAs, mechanical durability could be an issue under practical fuel cell operating conditions, where frequent humidity changes are involved. High Young's modulus of SPI membranes may cause high stress when hydrated.

We have reported that heterocyclic groups could improve the properties of SPI membranes. Triazole-containing SPI-8 membranes (see Fig. 1 for chemical structure) showed better water affinity and thus higher proton conductivity particularly at low humidity (or at low water content) compared to those of the conventional SPI copolymer membranes [15,16]. The SPI-8 membrane

* Corresponding authors at: Clean Energy Research Center, University of Yamanashi, 4 Takeda, Kofu, Yamanashi 400-8510, Japan. Tel.: +81 55 220 8707.
E-mail address: miyatake@yamanashi.ac.jp (K. Miyatake).

0378-7753/$ – see front matter © 2011 Elsevier B.V. All rights reserved.
doi:10.1016/j.jpowsour.2011.12.039

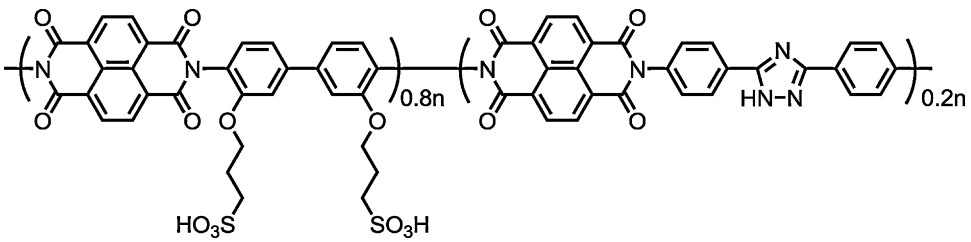

Fig. 1. Chemical structure of sulfonated polyimide copolymer (SPI-8).

was operable for 5000 h in hydrogen/air fuel cells at a constant current density of 200 mA cm^{-2} under high and low humidity conditions [17,18]. Chemical degradation was confirmed in the post-test membranes, however the degradation was not significant because of very low gas permeability of the SPI-8 membranes and small changes of the water content in the membranes during the operation.

The objective of the present research is to evaluate the durability of our SPI-8 membrane in humidity cycling test, in which the membrane is exposed periodically to dry (0% RH) and fully humidified (100% RH) conditions [19–21]. In the literature, there have been a few reports on the durability of hydrocarbon ionomer membranes in humidity cycling [22,23]. The experimental cell used in this study was the same as for practical fuel cells and the conditions were similar to the United States Department of Energy (US DOE) protocols [24] while some minor alternations were needed. Durability of the membrane was monitored by hydrogen permeation through the membrane. Post-test analyses by ^{1}H NMR spectra and molecular weight measurements were also carried out.

2. Experimental

2.1. Materials

Triazole-containing sulfonated polyimides (SPI-8) were synthesized according to the literature [15]. Five SPI-8 polymers with different degree of polymerization (molecular weight) were prepared by changing the comonomer ratios. Membranes in acid form were obtained by casting the SPI-8 solution in m-cresol, of which thickness was adjusted to be ca. 25 μm.

2.2. Measurements

Molecular weight measurement was performed via gel permeation chromatography (GPC) equipped with two Shodex KF-805 columns and a Jasco 875 UV detector set at 270 nm. *N*,*N*-Dimethylformamide (DMF) containing 0.01 M LiBr was used as the eluent at a flow rate of 1.0 mL min^{-1}. M_w and M_n were calibrated with standard polystyrene samples. Tensile strength was measured by a Shimadzu AGS-J 500N universal test machine attached with a Toshin Kogyo Bethel-3A temperature and humidity controllable chamber. Stress versus strain (SS) curves were obtained for samples cut into a dumbbell shape (DIN-53504-S3, 35 mm × 6 mm (total) and 12 mm × 2 mm (test area)). Measurement was conducted at 85 °C and 93% RH at a stretching speed of 10 mm min^{-1}. Reproducibility of SS curves was confirmed for each sample by repeating the measurement at least twice. The error in maximum stress and maximum strain was within 5% for all the tested samples. ^{1}H NMR spectra were obtained on a JEOL JNM-ECA 500 using deuterated dimethyl sulfoxide (DMSO-d_6) as the solvent and tetramethylsilane (TMS) as the internal reference, respectively.

2.3. Humidity cycling test

The SPI-8 membrane was sandwiched by two gas diffusion layers (GDLs, SGL Carbon Group Co., Ltd., 25BCH) and mounted into a single cell apparatus (Japan Automobile Research Institute (JARI) standard cell) consisting of two carbon separator plates with single serpentine flow fields. The size of the membrane contacting with the GDLs was 50 mm × 50 mm. The membrane with GDLs was compressed at 10 kgf cm^{-2} in the cell to ensure gas tight. The cell was operated at 80 °C flowing hydrogen into one side and argon into the other side at a flow rate of 100 mL min^{-1}, respectively. Humidity cycling was performed by alternating flow of dry (0% RH) gases for 2 min and fully humidified (100% RH) gases for 2 min, respectively. The humidities were monitored by a hygrometer placed at the inlet of the cell. The concentration of hydrogen permeated through the membrane was quantified with a Shimadzu GC-8A gas chromatography equipped with a thermal conductivity detector. The hydrogen permeability coefficient Q (cm^3 (STD) cm cm^{-2} s^{-1} cm Hg^{-1}) was calculated according to the following equations;

$$Q = \frac{273}{T} \times \frac{1}{A} \times B \times \frac{1}{t} \times l \times \frac{1}{76}$$

where T (K) is the absolute temperature of cell, A (cm^2) is the permeation area, B (cm^3) is the volume of the test gas permeated through the membrane, t (s) is the sampling time and l (cm) is the thickness of the membrane.

3. Results and discussion

3.1. Mechanical strength of the SPI-8 membranes

Unlike PFSA membranes, which may fail mechanically but not degrade chemically in humidity cycling, SPI membranes are more prone to degrade chemically (or depolymerize) via hydrolysis [15]. We therefore first clarified the relationship between molecular weight and mechanical strength in SPI-8 membranes. Five SPI-8 copolymers with different molecular weight were synthesized via polycondensation reaction of 3,3′-bis(sulfopropoxy)-4,4′-diaminobiphenyl (BSPA), 3,5-bis(4-aminophenyl)-1H-1,2,4-triazole (APTAZ), and 1,4,5,8-naphthalenetetracarboxylic dianhydride (TCND) [15]. Controlled excess of TCND provided SPI-8 copolymers with M_n = 42–122 kDa and M_w = 119–321 kDa (Table 1), as estimated by gel permeation chromatography (GPC) analyses. The polydispersity index (PDI = M_w/M_n) values were in the range of 2.4–2.8, typical for step growth polycondensation polymers. The degree of polymerization (n), defined as M_n divided by average molecular weight per repeat unit, was calculated to be 65, 75, 112, 154, and 188, respectively. The SPI-8s were soluble in polar organic solvents such as *m*-cresol and dimethyl sulfoxide (DMSO). Casting from *m*-cresol solutions provided brown and transparent membranes. The membranes were bendable and ductile even from the lowest molecular weight SPI-8(65).

Table 1
Molecular weight and mechanical properties of SPI-8 copolymer membranes used in this study.

Polymer[a]	M_w (10^3)	M_n (10^3)	PDI[b]	Maximum stress[c] (MPa)	Maximum strain[c] (%)
SPI-8(65)	119	42	2.8	21	3
SPI-8(75)	135	49	2.8	25	5
SPI-8(112)	177	73	2.4	21	8
SPI-8(154)	266	100	2.7	27	12
SPI-8(188)	321	122	2.6	31	16

[a] Degree of polymerization based on M_n in parenthesis.
[b] Polydispersity index (=M_w/M_n).
[c] Measured at 85 °C and 93% RH.

Mechanical properties of the SPI-8 membranes were evaluated by tensile strength measurement at 85 °C and 93% RH. The obtained SS curves are summarized in Fig. 2. A general trend was, as expected, that the higher molecular weight SPI-8 membranes showed better mechanical stability with higher maximum stress (at break point) and longer maximum strain. The maximum stress and strain of SPI-8(188) membrane were 31 MPa and 16%, respectively. There were approximate linear relationships between the degree of polymerization and the maximum stress/strain values as shown in Fig. 3. This is a useful finding since one can predict mechanical properties of the SPI-8 membranes from their molecular weight data.

3.2. Humidity cycling test

Humidity cycling test of SPI-8 membrane was carried out at 80 °C, simulating the practical fuel cell operating conditions. The US DOE protocol [24] suggests 90 °C (ca. 150% RH) for dew point of the wet gas to ensure fully hydrated state of membranes. It would require considerably high flow rate of dry gas (higher than several litters per min) to remove dew water and to dry membranes within a short period of time. We set at 80 °C (100% RH) for the dew point to enable short cycling period (4 min per cycle) with reasonable gas flow rate (100 mL min^{-1}). SPI-8(112) of middle molecular weight was chosen for the test. In Fig. 4 are shown changes in relative humidity (RH) and H_2 permeability coefficient during humidity cycling test of the SPI-8 membrane. The humidities of dry and wet gases were constant at 0% RH and 100% RH, respectively, as confirmed by a hygrometer placed at the inlet of the cell. The dry and wet conditions were maintained during 10,000 cycles of the test. The initial values of the hydrogen permeability coefficient were 1.0×10^{-10} (dry) and 7.2×10^{-9} (wet) cm^3 (STD) cm cm^{-2} s^{-1} cm Hg^{-1}, which were approximately corresponding to the values, 4.6×10^{-10} (0% RH) and 1.0×10^{-9} (90% RH) cm^3 (STD) cm cm^{-2} s^{-1} cm Hg^{-1}, obtained with a different gas permeability apparatus [15]. The results imply that the membrane is equilibrated with dry and wet conditions even in a shortened period of cycling period. The permeability coefficients increased during the cycling test, and reached 1.9×10^{-9} (dry) and 1.9×10^{-8} (wet) cm^3 (STD) cm cm^{-2} s^{-1} cm Hg^{-1} after 10,000 cycles. The measurement had to be discontinued at the cycle numbers of 1450 and 3810 due to the inevitable loss of electric power supply, which caused sudden drop and increase of the permeability. We have concluded that while the SPI-8 membrane showed minor increases in the H_2 permeability coefficient, the degradation was not significant without mechanical failure and pinholes. The results are rather surprising taking large water uptake (43 wt.% at 80% RH and 80 °C) and swelling of SPI-8 membrane [15]. SPI-8 membrane shows anisotropic swelling (ca. 3% in in-plane direction and ca. 210% in through-plane direction in water at 30 °C), which would be accountable for the durability in humidity cycling. The humidity cycling test was stopped at the cycle number of 10,370 to investigate the chemical and physical degradation of the membrane.

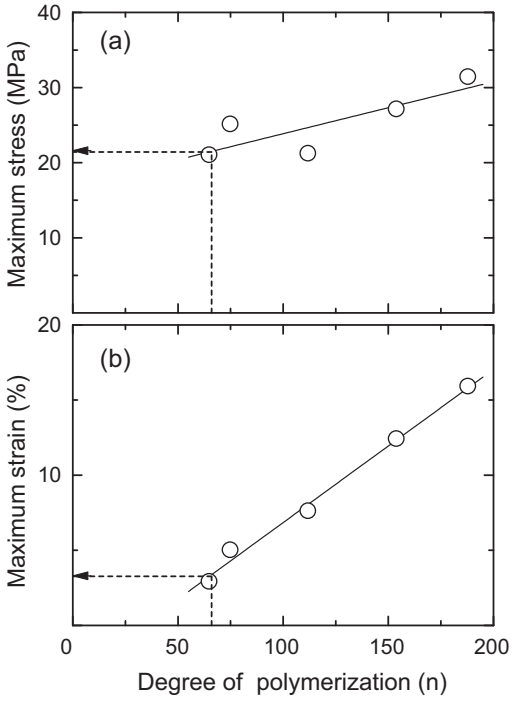

Fig. 3. (a) Maximum stress and (b) maximum strain of SPI-8 membranes as a function of degree of polymerization (n).

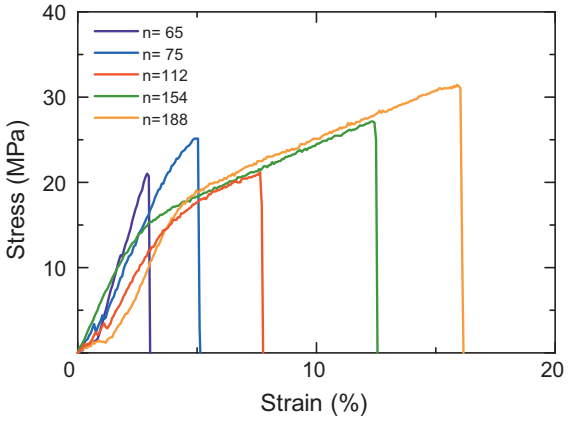

Fig. 2. Stress versus strain (SS) curves of SPI-8 membranes at 85 °C and 93% RH.

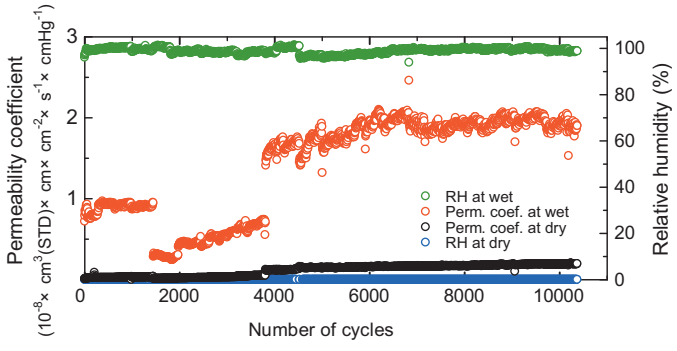

Fig. 4. H_2 permeability coefficient and relative humidity (RH) during humidity cycling test of SPI-8(112) membrane at 80 °C.

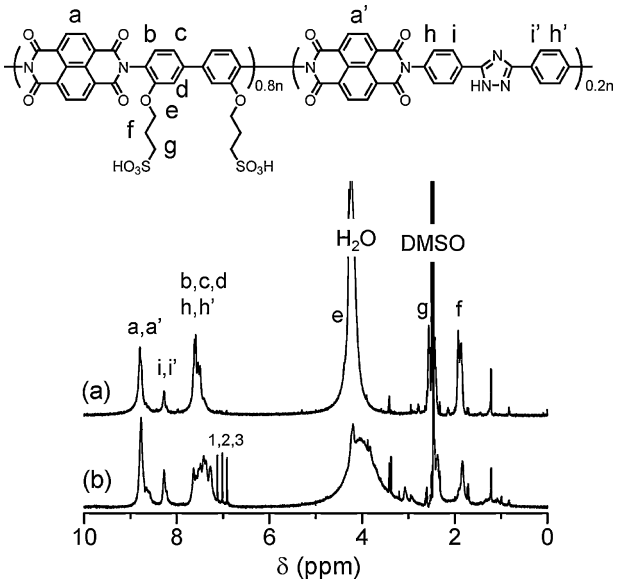

Fig. 5. ^{1}H NMR spectra of SPI-8(112), (a) pristine and (b) post-test samples.

3.3. Post-test analyses of the SPI-8 membrane

The cell was disassembled and the post-test membrane was recovered by removing the two gas diffusion layers (GDLs) carefully. The chemical degradation was investigated by ^{1}H NMR spectra. In Fig. 5 are compared ^{1}H NMR spectra of pristine and post-test SPI-8 membrane in deuterated dimethyl sulfoxide (DMSO-d_6) solution. The most significant differences were the peaks at 6.9–7.7 ppm of aromatic protons. The sharp three peaks appeared in the post-test sample were assigned to the hydroxyl-substituted phenylene rings attached to the imide groups (Fig. 6a), which suggested that some sulfopropoxy groups of the side chains were lost via hydrolysis. The ion exchange capacity (IEC) of the post-test membrane was calculated to be 2.19 meq g^{-1} from the integral ratio of the peaks, which was 11% lower than that (2.46 meq g^{-1}) of the pristine membrane. The post-test sample showed wide multiple peaks at 7.0–7.7 ppm due to the main chain degradation to provide amic acid structure (Fig. 6b) [25]. A small shoulder around 8.6 ppm implied the formation of naphthyl dicarboxylic acids via

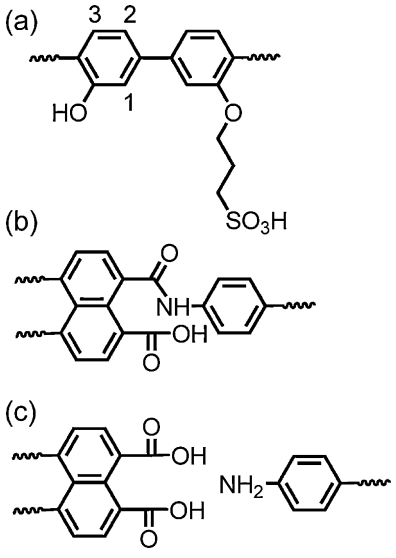

Fig. 6. Degradation products of SPI-8 via hydrolysis.

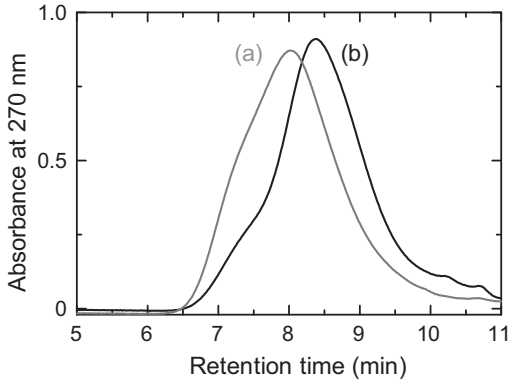

Fig. 7. GPC curves of SPI-8(112), (a) pristine and (b) post-test samples.

further hydrolysis of amic acid groups and the main chain scission (Fig. 6c) [26].

The degradation of SPI-8 was further confirmed by GPC analyses. The GPC profiles in Fig. 7 suggested that the post-test sample was of lower molecular weight than the pristine sample. The results are reasonable since both main chain and side degradations should cause lower apparent molecular weight. Molecular weight of the post-test sample was calculated to be M_w = 100 kDa and M_n = 43 kDa (n = 66). The loss of molecular weight was ca. 40%. While tensile strength measurement of the post-test membrane was not practically possible due to the physical damages when removing GDLs, the approximate linear relationships between molecular weight and maximum strain/stress in Fig. 3 enabled us to estimate the mechanical properties (the degraded products do not have the same molecular structure as the pristine membrane, however, the differences are rather minor at the end groups and hydroxyl groups and would not have significant effect on the GPC analyses). Dashed lines gave 3% of the maximum strain and 21 MPa of the maximum stress. The post-test SPI-8 membrane was assumed to retain high mechanical strength to suppress hydrogen permeation.

4. Conclusions

Durability of a non-fluorinated aromatic ionomer (sulfonated polyimide) membrane in humidity cycling has tested for fuel cell applications. The sulfonated polyimide copolymer membrane was durable during 10,000 wet/dry cycles without mechanical failure but with minor increase in hydrogen permeability. The hydrolytic degradation was confirmed with the post-test membrane by ^{1}H NMR and GPC analyses. The loss of ionic groups and molecular weight was 11% and 40%, respectively. Despite the hydrolytic degradation both in the main and the side chains, the sulfonated polyimide membrane retained high mechanical strength to have low hydrogen permeability. The anisotropic swelling behavior would be part of the reason for the high durability of the SPI-8 membrane in humidity cycling.

Acknowledgments

This work was partly supported by the New Energy and Industrial Technology Development Organization (NEDO) through the HiPer-FC Project, and the Ministry of Education, Culture, Sports, Science and Technology (MEXT) Japan through a Grant-in-Aid for Scientific Research (22760536, 23350089, and 23656427).

References

[1] A.J. Appleby, F.R. Foulkes, Fuel Cell Handbook, Van Nostrand Reinhold, New York, 1989.
[2] B.C.H. Steele, A. Heinzel, Nature 414 (2001) 345–352.
[3] A. Eisenberg, H.L. Yeager (Eds.), ACS Symp. Ser., No. 180: Perfluorinated Ionomer Membranes, 1982.
[4] A. Eisenberg, J.-S. Kim, Introduction to Ionomers, Wiley-Interscience, New York, 1998.
[5] M.A. Hickner, H. Ghassemi, Y.S. Kim, B.R. Einsla, J.E. McGrath, Chem. Rev. 104 (2004) 4587–4611.
[6] K. Miyatake, M. Watanabe, Electrochemistry 73 (2005) 12–19.
[7] E. Vallejo, G. Pourcelly, C. Gavach, R. Mercier, M. Pineri, J. Membr. Sci. 160 (1999) 127–137.
[8] J. Fang, X. Guo, S. Harada, T. Watari, K. Tanaka, H. Kita, K. Okamoto, Macromolecules 35 (2002) 9022–9028.
[9] X. Guo, J. Fang, T. Watari, K. Tanaka, H. Kita, K. Okamoto, Macromolecules 35 (2002) 6707–6713.
[10] N. Asano, M. Aoki, S. Suzuki, K. Miyatake, H. Uchida, M. Watanabe, J. Am. Chem. Soc. 128 (2006) 1762–1769.
[11] J. Yan, C. Liu, Z. Wang, W. Xing, M. Ding, Polymer 48 (2007) 6210–6214.
[12] T.J. Peckham, J. Schmeisser, M. Rodgers, S. Holdcroft, J. Mater. Chem. 17 (2007) 3255–3268.
[13] C. Marestin, G. Gebel, O. Diat, R. Mercier, Adv. Polym. Sci. 216 (2008) 185–258.
[14] Y.-S. Ye, Y.-J. Huang, C.-C. Cheng, F.-C. Chang, Chem. Commun. 46 (2010) 7554–7556.
[15] J. Saito, K. Miyatake, M. Watanabe, Macromolecules 41 (2008) 2415–2420.
[16] J. Saito, M. Tanaka, K. Miyatake, M. Watanabe, J. Polym. Sci. A: Polym. Chem. 48 (2010) 2846–2854.
[17] A. Kabasawa, J. Saito, H. Yano, K. Miyatake, H. Uchida, M. Watanabe, Electrochim. Acta 54 (2009) 1076–1082.
[18] A. Kabasawa, J. Saito, K. Miyatake, H. Uchida, M. Watanabe, Electrochim. Acta 54 (2009) 2754–2760.
[19] X. Huang, R. Solasi, Y. Zou, M. Feshler, K. Reifsnider, D. Condit, S. Burlatsky, T. Madden, J. Polym. Sci. B: Polym. Phys. 44 (2006) 2346–2357.
[20] H. Tang, S. Peikang, S.P. Jiang, F. Wang, M. Pan, J. Power Sources 170 (2007) 85–92.
[21] A. Kusoglu, A.M. Karlsson, M.H. Santare, S. Cleghorn, W.B. Johnson, J. Power Sources 170 (2007) 345–358.
[22] M.F. Mathias, R. Makharia, H.A. Gasteiger, J.J. Conley, T.J. Fuller, C.I. Gittleman, S.S. Kocha, D.P. Miller, C.K. Mittelsteadt, T. Xie, S.G. Yan, P.T. Yu, Electrochem. Soc. Interface 14 (2005) 24–35.
[23] Y.-H. Lai, C.K. Mittelsteadt, C.S. Gittleman, D.A. Dillard, J. Fuel Cell Sci. Technol. 6 (2009) 021002–021013.
[24] http://www1.eere.energy.gov/hydrogenandfuelcells/fuelcells/pdfs/component_durability_profile.pdf.
[25] C. Genies, R. Mercier, B. Sillion, R. Petiaud, N. Cornet, G. Gebel, M. Pineri, Polymer 42 (2001) 5097–5105.
[26] Y. Yin, Y. Suto, T. Sakabe, S. Chen, S. Hayashi, T. Mishima, O. Yamada, K. Tanaka, H. Kita, K.-I. Okamoto, Macromolecules 39 (2006) 1189–1198.